The Astrophysical Journal, 573:66–74, 2002 July 1

OPTICALLY FAINT COUNTERPARTS TO THE *INFRARED SPACE OBSERVATORY* FIRBACK 170 MICRON POPULATION: DISCOVERY OF COLD, LUMINOUS GALAXIES AT HIGH REDSHIFT

S. C. Chapman,[1] I. Smail,[2] R. J. Ivison,[3] G. Helou,[1] D. A. Dale,[4] and G. Lagache[5]

Received 2001 November 19; accepted 2002 March 7

ABSTRACT

We present Keck spectroscopy and UKIRT near-IR imaging observations of two 170 μm–selected sources from the *Infrared Space Observatory* (*ISO*) FIRBACK survey that have faint counterparts in the optical and $r-K \sim 5$. Both sources were expected to lie at $z > 1$, based on their far-infrared, submillimeter, and radio fluxes, assuming a spectral energy distribution similar to that of the local ultraluminous infrared galaxy (ULIRG) Arp 220. However, our spectroscopy indicates that the redshifts of these galaxies are less than 1: $z = 0.91$ for FIRBACK FN1-64, and $z = 0.45$ for FIRBACK FN1-40. While the bolometric luminosities of both galaxies are similar to that of Arp 220, it appears that the dust emission in these systems has a characteristic temperature of $\sim$30 K, much cooler than the $\sim$50 K seen in Arp 220. Neither optical spectrum shows evidence of active galactic nucleus activity. If these galaxies are characteristic of the optically faint FIRBACK population, then evolutionary models of the far-infrared background must include a substantial population of cold, luminous galaxies. These galaxies provide an important intermediate comparison between the local luminous IR galaxies and the high-redshift, submillimeter-selected galaxies, for which there is very little information available.

Subject headings: cosmology: observations — galaxies: evolution — galaxies: formation — galaxies: starburst

1. INTRODUCTION

The spectral shape of the far-infrared background (FIRB), detected by FIRAS at 100 μm–4 mm and DIRBE at 140 and 240 μm (Puget et al. 1996; Fixsen et al. 1998), indicates a peak at $\sim$200 μm, with energy comparable to the optical/UV background. This peak arises from optical/UV radiation from star formation and active galactic nucleus (AGN) activity in obscured galaxies at $z \gg 0$ that is absorbed by dust and reradiated in the far-infrared. This obscured population of galaxies might host approximately half of the massive star formation activity over the history of the universe (see, e.g., Blain et al. 1999).

Far-infrared surveys at wavelengths close to the peak of the FIRB provide a powerful route for understanding the properties of the obscured activity in the distant universe and its relevance to the formation and evolution of both galaxies and supermassive black holes. The FIRBACK (Far-Infrared Background; Dole 2000) survey obtained wide-field imaging at 170 μm with the PHOT instrument on board the *Infrared Space Observatory* (*ISO*) in three separate regions of the sky chosen for low Galactic cirrus foreground. FIRBACK is the most reliable and deepest [$\sigma(170\ \mu\text{m}) \sim 40$ mJy] infrared census at wavelengths near the peak in the FIRB. The FIRBACK sources down to 120 mJy account for about 10% of the FIRB seen by *COBE* at 140–240 μm (Puget et al. 1999). Evolutionary models (Dole et al. 2000; Lagache et al. 2002, in preparation) suggest that the sources identified by FIRBACK comprise both star-forming galaxies at low redshifts, $z \sim 0.1$, and a population of much more luminous galaxies at higher redshifts. The models predict that a quarter of the FIRBACK sources should have $z > 0.5$, with a tail reaching beyond $z = 1.5$. The sources in this high-redshift tail provide the strongest constraints on the evolution of the population contributing to the peak of the FIRB at $\sim$200 μm. For this reason, the identification and study of these galaxies is of particular interest (Sajina et al. 2002; D. Dennefeld et al. 2002, in preparation).

The coarse beam of *ISO* at 170 μm produces large uncertainties in the source positions (100″ diameter, 99% error circle). However, using the empirical radio-infrared correlation for star-forming galaxies (Helou, Soifer, & Rowan-Robinson 1985), we can exploit deep 1.4 GHz radio data from the VLA[6] in C configuration (Ciliegi et al. 1999) to identify the FIRBACK sources with positional uncertainties of only $\sim$1″ (15″ VLA beam size). Most FIRBACK sources lying within the sensitive region of the VLA image are detected in the radio (although some are not and are therefore difficult to identify at other wavelengths). Approximately 80% of the FIRBACK galaxies with radio identifications are detected in shallow sky surveys in the optical (second-generation Digital Palomar Observatory Sky Survey; DPOSS2) or near-IR (2MASS) (D. Dennefeld et al. 2002, in preparation). These 170 μm sources correspond to relatively low redshift galaxies ($z \sim 0.2$). The remaining 20% of the radio/FIRBACK N1 field population are identified in deep United Kingdom Infrared Telescope (UKIRT) K-band imaging at $17 < K < 21$ (Sajina et al. 2002). The faint near-IR magnitudes of these galaxies support the

[1] Department of Physics, California Institute of Technology, Pasadena, CA 91125.
[2] Department of Physics, University of Durham, South Road, Durham DH1 3LE, UK.
[3] Astronomy Technology Centre, Royal Observatory, Blackford Hill, Edinburgh EH9 3HJ, UK.
[4] Department of Physics and Astronomy, University of Wyoming, Laramie, WY 82071.
[5] Institut d'Astrophysique Spatiale, Université Paris Sud, Bâtiment 121, 91405 Orsay Cedex, France.

[6] The VLA is a facility of the National Radio Astronomy Observatory (NRAO). The NRAO is a facility of the National Science Foundation operated under cooperative agreement by Associated Universities, Inc.

existence of a high-redshift tail in the sample and provide an efficient route to identifying high-redshift candidates from the 170 μm population.

Additional constraints on the redshifts of the distant FIRBACK population are provided by submillimeter observations of a subsample of the catalog (Scott et al. 2000; A. Sajina et al. 2002, in preparation). SCUBA photometry observations at 850 μm, in conjunction with the 170 μm and 1.4 GHz fluxes, provide photometric redshift estimates (see, e.g., Carilli & Yun 2000). In this paper, we present Keck spectroscopy and UKIRT near-IR imaging observations of two FIRBACK sources, FIRBACK FN1 64 and FIRBACK FN1 40 (henceforth FN1 64 and FN1 40), which were detected by SCUBA in the submillimeter (Scott et al. 2000) and whose far-IR, submillimeter, and radio properties indicate they potentially lie at $z > 1$, in the high-redshift tail of the FIRBACK distribution. Our calculations assume a flat, $\Lambda = 0.7$ universe and $H_0 = 65$ km s^{-1} Mpc^{-1}, providing a scale of 8.4 kpc arcsec^{-1} at $z = 0.91$ (FN1-64) and 6.2 kpc arcsec^{-1} at $z = 0.45$ (FN1-40).

2. OBSERVATIONS

The initial identification of the FIRBACK sources involves searching for optical counterparts in the DPOSS2 *F*-band images (close to Gunn *r*) of this region, using the accurate positions of the sources from the radio maps. This search highlights both FN1-40 and FN1-64 as optically faint (or undetected) sources, at the limit of DPOSS2 (and also of the available CCD imaging; D. Dennefeld et al. 2002, in preparation).

The sources are expected to be at $z > 1$, based on photometric redshifts from the FIR/submillimeter/radio. Using the standard Carilli & Yun (2000) estimator for radio/850 μm gives $z_{\rm FN1\text{-}40} = 1.1$ and $z_{\rm FN1\text{-}64} = 1.3$, with a 1 σ uncertainty of 0.17. Aperture-matching the observations at different wavelengths (radio, 15″; 850 μm, 19″; 450 μm, 11″; 170 μm, 100″) could introduce errors in such redshift estimates, with confusion problems particularly affecting the 170 μm band.

To provide complete, high-resolution, *K*-band identifications for the FIRBACK sources, a campaign is underway involving deep near-IR imaging (S. C. Chapman et al. 2002, in preparation).

2.1. *UKIRT Imaging*

We observed FN1-40 and FN1-64 in the *K* band at UKIRT using the Fast Track Imager (UFTI) as part of the ongoing identification campaign of FIRBACK sources. The source positions were taken from the radio/SCUBA identifications as uncovered in Scott et al. (2000), with coordinates listed in the catalog of Dole et al. (2000). Each source was imaged for a total of 1800 s, with individual exposures of 60 s, reaching a limiting magnitude in a 2″ diameter aperture of $K = 20.4$ (5 σ) in 0.″4 seeing. Data were reduced using the UKIRT software pipeline ORACDR (Bridger et al. 2000).

The *K*-band imaging of both sources is shown in Figure 1. The precise mapping of the radio source catalog onto the optical grid suggests that the astrometric error is dominated by the centroiding of the radio sources themselves [FWHM$_{1.4\ \rm GHz}$/2(S/N) $\sim$ 1″]. The UKIRT observations clearly identify near-IR counterparts at the position of the radio source in both cases. Indeed, we find several near-IR components close to the radio counterpart, on scales of $<$5″ (less than 50 kpc at $z < 1$). These components are all resolved in 0.″4 seeing, confirming that they are all galaxies.

Based on the available optical limits, we find that in both sources the component that is coincident with the radio emission, and by implication is the source of the luminous far-IR emission, is very red, $r-K \sim 5$ (Table 1).

TABLE 1
PROPERTIES OF FIRBACK FN1-64 AND FN1-40

Property	FN1-40	FN1-64
R.A. (J2000.0)	16 09 28.01	16 08 25.33
Decl. (J2000.0)	54 28 32.6	54 38 09.5
Redshift$_{\rm spec}$	0.449 ± 0.003	0.907 ± 0.001
Redshift$_{\rm phot}$	1.1 ± 0.2	1.3 ± 0.2
U[a] (mag)	$>24.4/>24.4$	$23.30/>24.6$ (21.28)
g[a] (mag)	$>24.7/>24.7$	24.33/23.10 (21.91)
r[a] (mag)	24.45/24.57	23.48/22.52 (21.37)
i[a] (mag)	23.96/23.81	21.64/20.75 (19.93)
z'[a] (mag)	22.31/22.40	20.09/19.82 (18.83)
K[a] (mag)	19.73/20.51	18.63/18.71 (18.15)
$S_{170\ \mu\rm m}$ (mJy)	204.7 ± 44.6	166.2 ± 42.0
$S_{450\ \mu\rm m}$ (mJy)	42.0 ± 29.5	49.7 ± 19.4
$S_{850\ \mu\rm m}$ (mJy)	6.3 ± 1.4	5.9 ± 1.4
$S_{20\ \rm cm}$ (μJy)	330 ± 30	230 ± 40
$L_{\rm FIR}$[b]	6.7×10^{11}	4.0×10^{12}
$L_{\rm TIR}$[c]	1.6×10^{12}	7.7×10^{12}
[O II] 3729/3726	1.45	0.72
Hα/Hβ	9.54	...
[O III] 5007/[N II] 6584	1.66	...
Hγ/Hβ	<0.2	0.24
R_{23}	6.27	3.56
[O III] 4959 + 5007/[O II]	0.61	0.95
SFR (Hβ) (reddening-corrected) ($M_\odot$ yr^{-1})	20	416
SFR (far-IR) ($M_\odot$ yr^{-1})	160	950
FIR/Opt[d]	36.2	20.7
60 μm/100 μm (rest-frame)	0.43	0.69

NOTE.—Units of right ascension are hours, minutes, and seconds, and units of declination are degrees, arcminutes, and arcseconds.

[a] Quantities with divisions are quoted for components J1 and J2, respectively. Magnitudes are calculated for 2″/2″ apertures (for J1/J2). Quantities in brackets are for the total system in the case of the obviously merging FN1-64. Photometry limits (3 σ) are (U, g, r, i, z', K) = (24.4, 24.7, 24.6, 23.9, 22.4, 20.5).

[b] $S_{\rm FIR} = (1.26 \times 10^{-14})(2.58 S_{60} + S_{100})$ W m^{-2}; $L_{\rm FIR}$ computed using a flat, $\Lambda = 0.7$ cosmology.

[c] $L_{\rm TIR}$ covers 3–1100 μm, as defined in Dale et al. 2001.

[d] The *obscuration* ratio between FIR luminosity and optical/near-IR luminosity, as described in the text.

2.2. *Archival Isaac Newton Telescope Imaging*

Archival multiband data are made publicly available through the Isaac Newton Group's Wide Field Camera Survey Programme. We extracted *U*-, *g*-, *r*-, *i*-, and *z'*-band imaging for our FIRBACK galaxies, stacking multiple exposures in the same filters with IRAF IMCOMB. The imaging has 0.″33 pixel^{-1}, with an average 1.″2 FWHM point-spread function (PSF). The calibration zero points were taken from the archive listing for the appropriate observation date.[7] Figure 1 shows these images scaled to the

[7] See http://www.ast.cam.ac.uk/~wfcsur/photom.html.

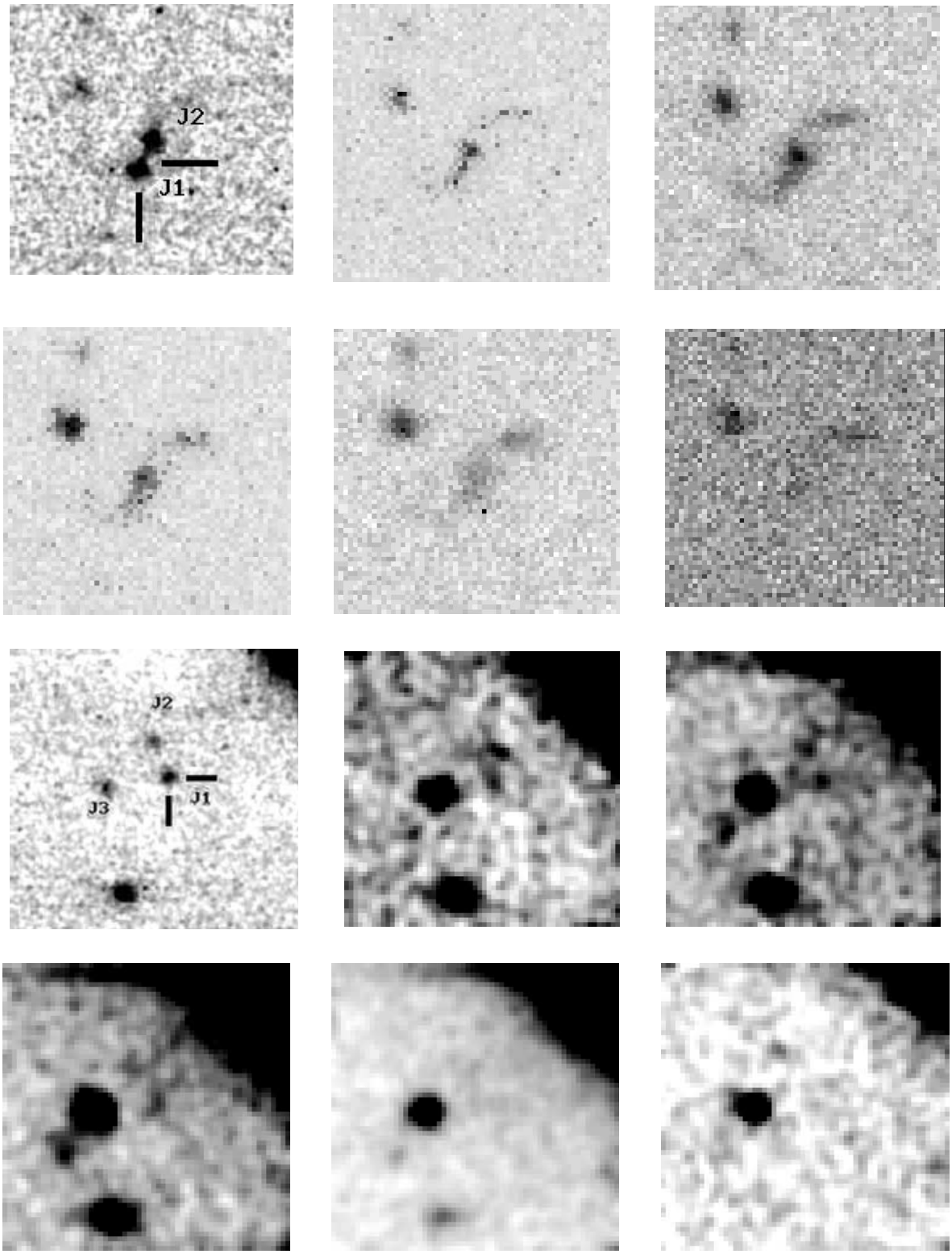

FIG. 1.—Multiband images of FN1-64 ($z = 0.91$; *top two rows*) and FN1-40 ($z = 0.45$; *bottom two rows*), used to identify the FIRBACK population (NET archive), and our deep UKIRT *K*-band imaging, which reliably identifies the counterparts to these two sources. In each pair of rows, the top row shows *K*, z', and *i* images and the bottom row *r*, *g*, and *U* images (*left to right*). The data for the fainter FN1-40 have been smoothed with the PSF for visibility. The seeing at UKIRT was $0''.4$, providing a high-resolution view of these luminous dusty galaxies. The radio source position is shown by the crosshair and in each case is coincident with a very red ($r-K \sim 5$) galaxy component. We identify several components in each source (major components labeled J1, J2, and J3) and conclude that both galaxies likely show a multicomponent merging structure reminiscent of local ULIRGs. Each panel is $20''$ on a side, with north up and east to the left.

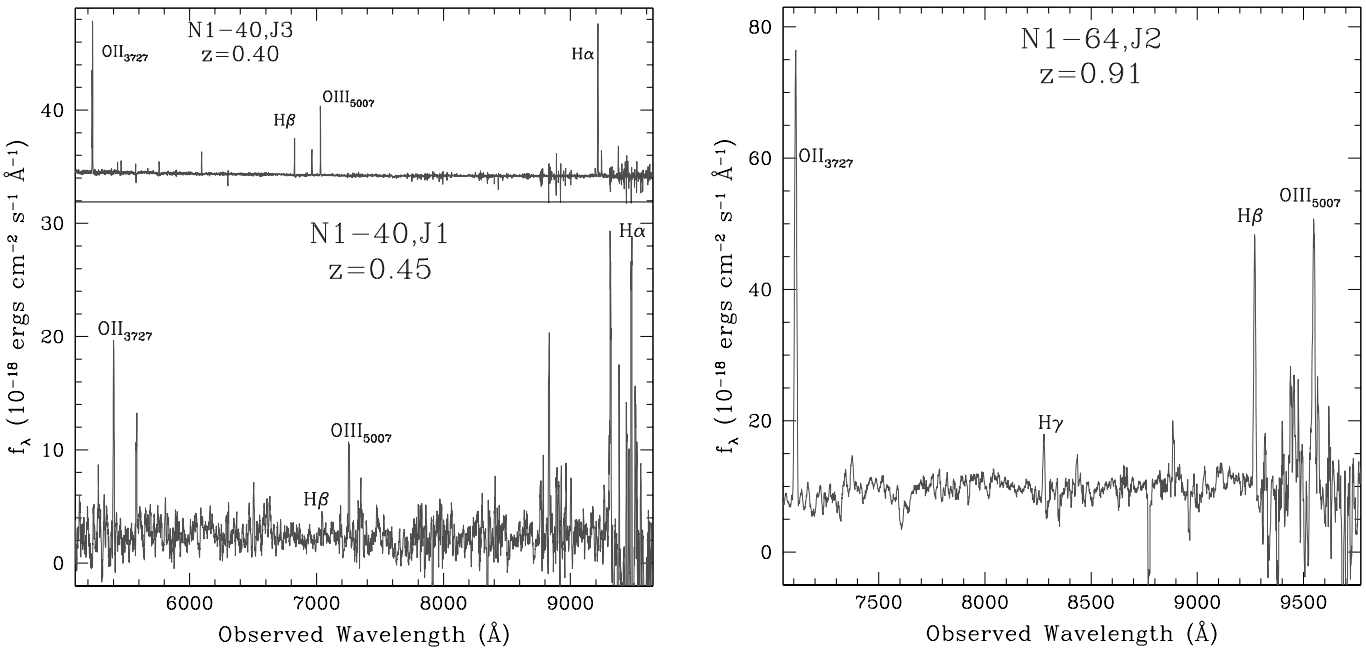

FIG. 2.—Keck/ESI spectra of FN1-40 (*left*), with the radio-identified source J1 at $z = 0.45$. Inset for comparison is the optically bright component J3 ($z = 0.40$) lying on the same slit, with flux scaled down by 100 times. While they are relatively close in redshift, the velocity difference ($\sim$13,000 km s^{-1}) is too large for them to be part of the same merging system. The Balmer ratios do not show any significant reddening. FN1-64/J2, the optically brighter component of an obviously merging pair, is presented at right ($z = 0.91$). Detected lines are indicated. Spectral resolution is $\sim$1 Å, resolving the [O II] doublet in all cases.

UKIRT frame. FN1-64 displays a striking merger morphology, with components spanning a range in spectral energy distributions (SEDs). The strong *K*-band J1 component appears only as a faint tail in the optical. FN1-40 is a much fainter optical source, and we have smoothed the image with the PSF for display purposes. Some faint emission between J1 and J2 in the *I* and z' images suggests that this source may also be an interaction between multiple components. We find that in both sources the component that is coincident with the radio emission, and by implication is the source of the luminous far-IR emission, is very red, $r-K \sim 5$ (Table 1).

2.3. *Keck Spectroscopy*

Having identified reliable counterparts to the 170 μm sources in these two fields, we are thus in a position to test the prediction that these galaxies should lie at $z > 1$.

Spectroscopic observations of FN1-40 and FN1-64 were taken using the Echellette Spectrograph and Imager (ESI) on the Keck II telescope in 2001 July. In the echellette mode used here, ESI provides complete coverage of the optical wave band from the atmospheric cutoff to the limit of the sensitivity of silicon CCDs: 0.32–1 μm. The high spectral resolution of the system, $\sim$1 Å, allows for very good sky subtraction into the atmospheric OH forest at the red end of the spectrum.

The galaxies were acquired and centered on the slit manually using the optical guide camera. In the case of FN1-40, we were able to center on the bright galaxy, J3 (Fig. 1), with the slit aligned to cover J1, the component identified with the radio emission. For FN1-64, only the optically brighter component of the merging pair, J2, was aligned on the slit.

The spectral integrations were 1800 s for each source. High signal-to-noise ratio flats and wavelength calibrations were taken shortly before the observations of each target, and fluxes were calibrated using spectra of red standard stars. The data were reduced with the MAKEE software, using the standard reduction recipe outlined in the manual (Bridger et al. 2000). The calibrated spectra for FN1-40/J1 and FN1-64/J2 (as well as for the acquisition object FN1-40/J3) are shown in Figure 2.

The spectra of both FN1-40/J1 and FN1-64/J2 show a series of strong emission lines in the red. We identify the strongest of these as [O II] 3727, [O III] 5007, and, for FN1-40, Hα. Based on these identifications, we determine redshifts of $z = 0.45$ for FN1-40/J1 and $z = 0.91$ for FN1-64/J2.[8] In addition, we measure a redshift of $z = 0.40$ for the acquisition galaxy, J3, in the field of FN1-40. More details of the spectral line strengths from these observations are given in Table 1.

3. RESULTS

The ESI spectroscopic observations provide reliable redshifts for the proposed radio-detected counterparts to the 170 μm sources in the fields of FN1-40 and FN1-64. These redshifts, $z = 0.45$ and $z = 0.91$, respectively, are below those predicted on the basis of the far-IR, submillimeter, and radio properties of these galaxies, assuming an SED for these luminous, dusty galaxies similar to that of Arp 220. We now investigate this discrepancy in more detail.

[8] For completeness, we note that an attempt to detect redshifted Hα in FN1-64/J2, using an 1800 s *J*-band observation with the CGS4 spectrograph on UKIRT, failed to detect a line at the relevant wavelength.

3.1. *Far-IR Properties*

Figure 3 depicts the measured near-IR through radio photometry for the two FIRBACK galaxies. A template fit from the SED library of Dale et al. (2001; Dale & Helou 2002) is overlaid, encompassing the mid-IR through radio wavelengths. This template library represents a parameterized sequence of SEDs (ordered in terms of their 60 μm/100 μm rest-frame flux ratios) in which a range of dust properties (temperatures and emissivities) are modeled to provide a composite SED, with increasing far-IR colors for increasing far-IR luminosity. These SEDs provide a good representation of all local, far-IR, luminous galaxies (Dale et al. 2001; Dale & Helou 2002). The radio luminosity of the model SED is tied directly to the far-IR luminosity, using the empirical relation from Helou et al. (1985).

To fit these models to our observations, we simply minimize χ^2 between the SED and the observations for the radio through far-IR points, ignoring the poor signal-to-noise ratio 450 μm point and weighting each of the points equally. In the case of FN1-64, the Dale et al. templates cannot simultaneously fit the radio, 850 μm, and 170 μm bands to within the 1 σ uncertainties; however, the fit lies within the 0.2 dex scatter of the FIR-radio relation (Helou et al. 1985). For reference and illustration, we also show the best fit excluding the 170 μm point. The excellent resulting fit, with a slightly cooler template (lower 60 μm/100 μm parameter), to the 450 μm, 850 μm, and radio points suggests that the large *ISO*/PHOT beam (100″ diameter, 99% error circle) may include another far-IR source, in addition to the one isolated by the radio and submillimeter. A second radio source, with $S_{1.4\ \mathrm{GHz}} < 5\ \sigma$ (Ciliegi et al. 1999), lies toward the edge of the FIRBACK error circle and may be contributing to the FIR flux.

From our fits we estimate that the galaxies are relatively cool, with rest-frame 60 μm/100 μm ratios of 0.43 ± 0.03 and 0.69 ± 0.04 for FN1-40 and FN1-64, respectively, where flux errors lead to an uncertainty in the 60 μm/100 μm ratio of the fit. As the Dale et al. SED models assume a superposition of blackbodies of different temperatures, they can be described best in terms of percentage of L_{IR} contributions from dust at different temperatures. For $T_d < 15$ K, <20 K, and <31 K, FN1-40 has, respectively, 42%, 89%, and 100%, while FN1-64 has 31%, 78%, and 98%. However, for direct comparison with other galaxies from the literature, we also fit a single dust temperature and emissivity (β) to the submillimeter/far-IR data points and obtain $T_d = 25.7 \pm 0.4$ K, with $\beta = 1.76 \pm 0.01$, for FN1-40 and $T_d = 30.8 \pm 0.7$ K, with $\beta = 1.68 \pm 0.02$, for FN1-64. These values of β lie within the 1 σ range of local values for *IRAS* galaxies, as fitted by Dunne et al. (2000) (median $\beta = 1.33$). We consider the effects of dust temperature further in subsequent sections.

In terms of bolometric far-IR luminosity (40–200 μm), using the best-fitting SEDs we estimate that FN1-40 has a luminosity of $L_{\mathrm{FIR}} \sim 7 \times 10^{11}\ L_{\odot}$, placing it just in the ULIRG category. FN1-64 is more luminous, with $L_{\mathrm{FIR}} \sim 4 \times 10^{12}\ L_{\odot}$, placing it well into the ULIRG class and showing that it is 4 times as luminous as Arp 220. In both cases, adopting total infrared luminosities, L_{TIR}, covering all the emission from 3 to 1000 μm in the rest frame, we estimate luminosities that are $\sim$2 times higher than the corresponding L_{FIR}.

We compare, in Figure 4, the rest-frame 60 μm/100 μm ratios (corresponding roughly to dust temperature) and

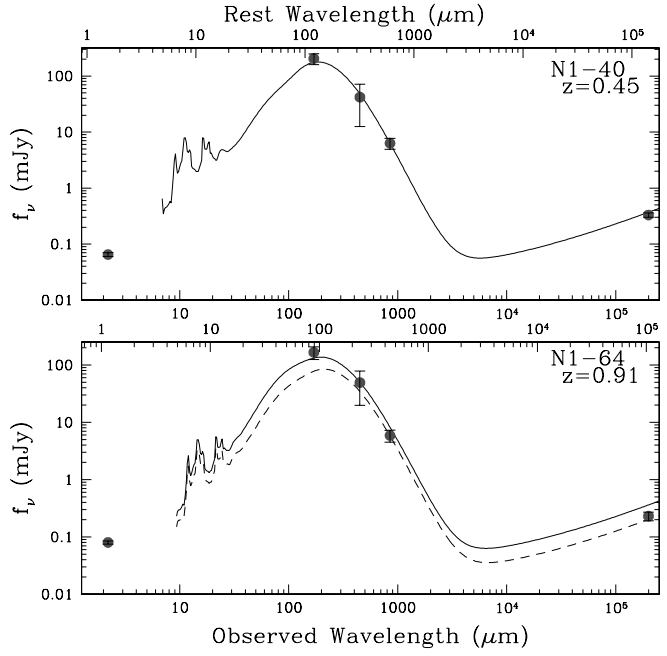

FIG. 3.—Observed SEDs of FN1-40 (*top*) and FN1-64 (*bottom*) from optical through radio measurements. The best-fit models from the catalog of Dale et al. (2001) are overlaid, illustrating the colder nature of FN1-40 at $z = 0.45$. FN1-64 has hotter dust but is still relatively cool compared to Arp 220 (a ULIRG that has only $\frac{1}{4}$ the bolometric luminosity of FN1-64). For FN1-64, a simultaneous fit to 170 μm, 850 μm, and 1.4 GHz is rather poor, and an improved, cooler dust fit to the 450 μm, 850 μm, 1.4 GHz bands is shown as a dashed line (motivated by the possibility of an additional source of far-IR emission contributing to the large *ISO* FIRBACK beam).

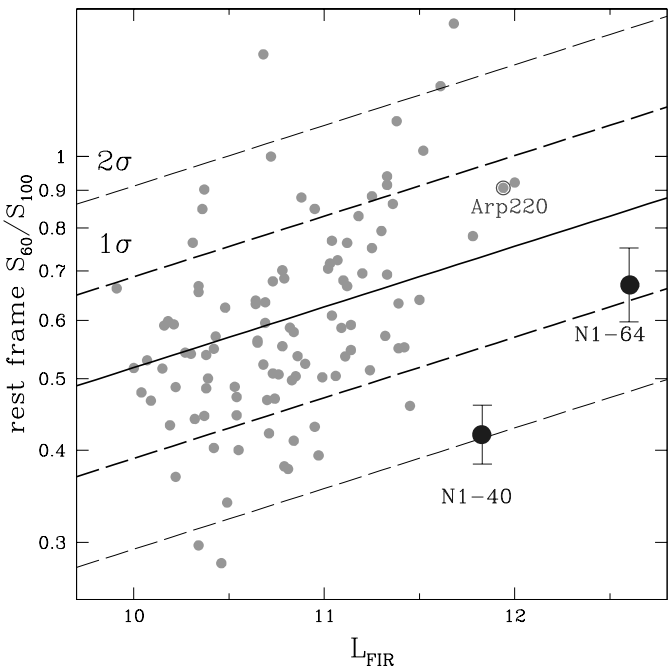

FIG. 4.—Dependence of rest-frame 60 μm/100 μm ratio (roughly, dust temperature) with L_{FIR} for the Dunne et al. (2000) SCUBA-observed sample of BGS *IRAS* sources, compared with our two FIRBACK galaxies. Error bars denote the model-fitting error from photometric uncertainties. The correlation and 1 and 2 σ deviations are overlaid. Arp 220, the ULIRG typically used for comparison with high-z luminous galaxies, is identified.

FIR luminosities for these FIRBACK galaxies with those of a subsample of the *IRAS* Bright Galaxy Sample (BGS) with 850 μm measurements (Dunne et al. 2000). Our extrapolation to 60 μm/100 μm ratios is somewhat model-dependent; while our observed 170 μm point measures the rest-frame 100 μm flux, our model fitting gives a variation in the 60 μm point, dominated by photometric uncertainties (shown with error bars in Fig. 4). Fitting single dust temperature graybodies to local *IRAS*-selected galaxies using the 850 μm point (Dunne et al. 2000) has demonstrated that using the 60 μm/100 μm ratio alone slightly overestimates T_d, with T_d showing a tighter correlation than the 60 μm/100 μm ratio with $L_{\rm FIR}$. This comparison shows that these two FIRBACK galaxies are colder than the majority of the *IRAS* BGS, given their $L_{\rm FIR}$. However, the BGS ($S_{60\ \mu{\rm m}} > 5.24$ Jy) is relatively small, with very few objects as luminous as FN1-40 and FN1-64. We would like to make a comparison with the fainter $S_{60\ \mu{\rm m}} > 1.2$ Jy *IRAS* galaxies (Fisher et al. 1995). The local 60 μm/100 μm ratio distribution of the 1.2 Jy sample is characterized in detail in S. C. Chapman et al. (2002, in preparation). Placing the two FIRBACK galaxies within their respective far-IR luminosity classes, we find that FN1-40 lies midway into the first quartile of 60 μm/100 μm ratio values for $L_{\rm FIR} \sim 10^{11.6}$, while FN1-64 lies at the first quartile point for $L_{\rm FIR} \sim 10^{12.1}$. This is roughly consistent with the extrapolated relation for the BGS shown in Figure 4. We discuss the implications of this discovery in § 4.

3.2. *Optical Properties and Morphologies*

The existing optical imaging (1.″2 FWHM) reveals an obviously merging, $r = 21.4$, elongated source for FN1-64 and barely detected $r \sim 24.5$ components for FN1-40. Our 0.″4 UKIRT imaging in the *K* band, however, provides significant morphological information (Fig. 1).

The *K* image of FN1-64 resolves into a pair of galaxies with approximately equal *K*-band flux, and the complete system has a $K = 18.15$. However, only the northern *K*-band source has a bright optical counterpart, with only a faint $r = 23.5$ tail corresponding to the southern source. Hence, this pair comprises a blue component to the north and a red ($r-K \sim 5$) galaxy in the south. The latter is coincident with the radio emission and by implication is probably generating the bulk of the far-IR output. The galaxies are separated by 2.″4, which translates into 20 kpc at $z = 0.91$, and there is a bridge of emission connecting the two components, suggestive of tidal debris.

FN1-40 is a faint galaxy ($r = 24.5$), with a possible close companion at 2.″3 separation (J2) and a third, optically bright galaxy (J3) lying 3.″6 away from J1. The radio centroid is coincident with component J1, the *K*-brightest source with $r-K = 4.8$, as labeled in Figure 1. Our spectrum identifies this as a galaxy at $z = 0.45$. As the J3 source ($z = 0.40$) has a velocity offset of $\sim$13,000 km s^{-1} from J1, it cannot be considered a part of the system. Both J1 and J2, however, show low surface brightness extension (especially in the z' and *i* images) along the axis separating the two components, and we suggest that this probably represents a merging system.

A comparison of the morphologies of these two FIRBACK sources, multiple components separated on scales of $\sim$10 kpc, with local ULIRGs (Goldader et al. 2002) suggests a similarity with "early-stage mergers," such as VV 114. Equally, the tendency for the radio emission (and therefore, presumably, the far-IR) to come from the redder component is also shared with local ULIRG samples. However, there are differences. The far-IR curves for FN1-40/FN1-64 are fitted by cool SEDs, which would normally be accompanied by a modest $L_{\rm FIR}/L_{\rm optical}$ ratio for such early-stage mergers (Dale et al. 2001). In contrast, the measured $L_{\rm FIR}/L_{\rm optical}$ ratio, considering both the J1 and J2 components in each case, is large (36.2 and 20.7 for FN1-64 and FN1-40, respectively). The $L_{\rm optical}$ is calculated from the integrated flux under a power-law fit to rest-frame wavelengths 0.35–1.50 μm. These values are similar to those for Arp 220, a more evolved ULIRG with a hotter dust temperature ($\sim$50 K).

3.3. *Spectral Properties and Metallicities*

Combinations of strong emission lines can be used to determine or constrain the nature of the ionizing radiation (Veilleux & Osterbrock 1987), the amount of reddening to the emission region, and the metallicity of the interstellar medium (ISM; see, e.g., Pagel et al. 1979; Kobulnicky, Kennicutt, & Pizagno 1999). It is important to stress that these measurements only reflect the environment from which photons can escape, and it is possible that the most active regions within these systems are so highly obscured that they do not contribute to the optical spectra used in our analysis. Moreover, in the case of FN1-64/J2, our optical spectrum is offset from the very red object, radio-emitting component of the system (although this has not traditionally limited the analysis of other, similar systems; see, e.g., Ivison et al. 2001).

The narrow lines and the resolution of the [O II] doublet in both systems suggest that no AGN component is present in either FN1-64/J2 or FN1-40/J1, although without direct spectroscopic information from the far-IR–dominant region of FN1-64/J2, we cannot rule out an AGN origin within this component (J1). The optical spectra of both FN1-64/J2 and FN1-40/J1 resemble those of luminous H II regions.

For FN1-40/J1, we can calculate the optical reddening based on the Balmer ratio, Hα/Hβ. The region emitting Balmer lines is apparently highly reddened, equivalent to an $A_V = 3.6$ mag and consistent with the copious far-IR emission being centralized in the same location as the optically brighter region for which the spectra diagnostics have been measured. Applying this extinction to the Hβ-inferred star formation rate (SFR) suggests a correction from 0.7 to 20 $M_\odot$ yr^{-1}, still well below that extrapolated from the far-IR (160 $M_\odot$ yr^{-1}). We are able to probe the extinction in FN1-64/J2 through the Hβ/Hγ, revealing a more modest $A_V = 2.1$. As stressed above, this constraint is not for the major source of far-IR emission in this system (J1). However, the Hβ-implied SFR from J2 (416 $M_\odot$ yr^{-1}) is comparable to the far-IR–derived SFR from J1 (950 $M_\odot$ yr^{-1}). The FN1-64 system is therefore reminiscent of other high-z ULIRGs for which the optically bright component provides an insight into the luminosity of the obscured portion (see, e.g., Ivison et al. 2001; see § 4 for further examples).

To measure the ISM metallicity, a rigorous determination requires knowledge of electron temperature derivable only from intrinsically weak lines. However, metallicity diagnostic line ratios based on stronger lines have been empirically calibrated. In particular, the R_{23} parameter, $R_{23} = ([{\rm O\ II}]\ 3727 + [{\rm O\ III}]\ 4959 + 5007)/{\rm H}\beta$ (Pagel et al.

1979), has been calibrated against metallicity, with an intrinsic scatter of only 0.2 dex. It is a weak function of the ionization ratio [O III] 4959+5007/[O II] 3727. A reversal in R_{23} occurs at $Z \sim 0.3\ Z_{\odot}$ as a result of cooling effects, so a low- and a high-metallicity solution are associated with most values of R_{23}. This degeneracy can, however, be broken using the [O III] 5007/[N II] 6584 ratio (Kobulnicky et al. 1999).

The metallicity can be used as an indicator of a galaxy's evolutionary state and as a constraint on possible present-day descendants. Carollo & Lilly (2001) have investigated the ISM metallicities of Hβ-luminous field galaxies in the $0.5 < z < 1.0$ redshift interval from the Canada-France Redshift Survey (CFRS). These galaxies fall in the R_{23} versus [O III]/[O II] plane in locations that are occupied by galaxies in the local Jansen et al. (2000) sample. At both epochs, galaxies selected to have the same Hβ luminosities exhibit the same range of R_{23} and [O III]/[O II]. We find that the galaxies FN1-40/J1 and FN1-64/J2 are within our 1 σ error of the median properties of the CFRS sources in the [O III] 4959+5007/[O II] 3727 versus R_{23} plane. For the lower redshift FN1-40 source, we can use the detected [N II] 6584 to break the metal degeneracy of the R_{23} indicator. The [O III] 5007/[N II] 6584 < 2 necessitates metallicities $Z > 0.5\ Z_{\odot}$, placing the source on the upper branch of the relation, with a metallicity close to the solar value.

While the Carollo & Lilly (2001) galaxies in the $0.5 < z < 1.0$ range are bright, star-forming galaxies, they fall an order of magnitude below the bolometric luminosity of our two FIRBACK sources under study (several Carollo & Lilly 2001 galaxies are detected in the CFRS 15 μm *ISO* sample of Flores et al. 1999). While it is therefore interesting to compare R_{23} metallicities for these objects, we stress that the R_{23} indicator has only been calibrated for low-obscuration regions and may not be a valid surrogate for metallicity in the highly obscured environments of ULIRGs. In particular, we are only measuring R_{23} from regions that happen to be visible, from a system that is likely to be generally obscured.

4. DISCUSSION

At $z < 1$, sources observed at both 170 and 850 μm will exhibit similar characteristics as a function of dust temperature (Blain 1999); the coldest and most dusty galaxies will have the greatest flux densities for an equivalent far-IR luminosity. Beyond $z \sim 1$, the 170 μm band lies blueward of the peak in the rest-frame black body, and dust temperatures $T_d < 100$ K no longer have significant effects on the observed source flux. A flux-limited survey, such as FIRBACK, is thus expected to be biased toward cooler galaxies at higher redshifts. While we do not yet have the statistics to quantify the actual selection rate, we note that the identification of the unusually cold ULIRGs FN1-40 and FN1-64 is in agreement with this prediction: we find galaxies cooler than expected for the $\sim 10^{12}\ L_{\odot}$ bolometric luminosities.

Models of the FIRBACK population (Dole et al. 2000) have evolved the local luminosity function by boosting only the ULIRG contribution with redshift, assuming an average SED template for ULIRGs. This scenario is able to fit the FIRB and the FIRBACK counts, implying that 30% of these sources lie at $0.5 < z < 1.0$ and 10% at $1 < z < 2.5$ (Dole et al. 2000). However, the assumption that an average ULIRG template can represent the FIRBACK source population is flawed, as it does not take into account the much colder sources that will be preferentially selected at 170 μm for $z < 1$. Other recent models of the far-IR galaxy population (Franceschini et al. 2001; Chary & Elbaz 2001) do not incorporate a cold luminous galaxy template and cannot directly account for numerous sources, such as FN1-40 and FN1-64. Revisions to the Dole et al. model (Lagache et al. 2002, in preparation) include a population of colder, luminous objects based on the SED shape of the less luminous local FIRBACK sources.

The actual redshifts of both FN1-40/FN1-64 ($z = 0.45$ and 0.91, respectively) lie significantly below the $z = 1.1$ and 1.3 predicted from the submillimeter and radio using the Carilli & Yun (2000) estimator (with 1 σ uncertainty of 0.17), which is also derived from the average ULIRG SED. Moreover, if the majority of FIRBACK sources were to span the range in properties observed in these two galaxies, the average properties deduced from an Arp 220 template would be severely skewed to higher redshifts. We chose these two sources for Keck follow-up at random from the FIRBACK sources for which the submillimeter/radio ratio suggested a high ($z > 1$) redshift. As a consequence, the distinct possibility exists that almost none of the radio-identified FIRBACK sources may lie at $z > 1$, depending on the mid- and high-redshift distributions in dust temperature.

The measurement of the 850 μm/1.4 GHz ratio for both these sources does allow a constraint on its use as a redshift indicator. Clearly, the ratio for these sources must lie significantly above the canonical value for ULIRGs found by Carilli & Yun (2000), as shown in Figure 5. The existence of

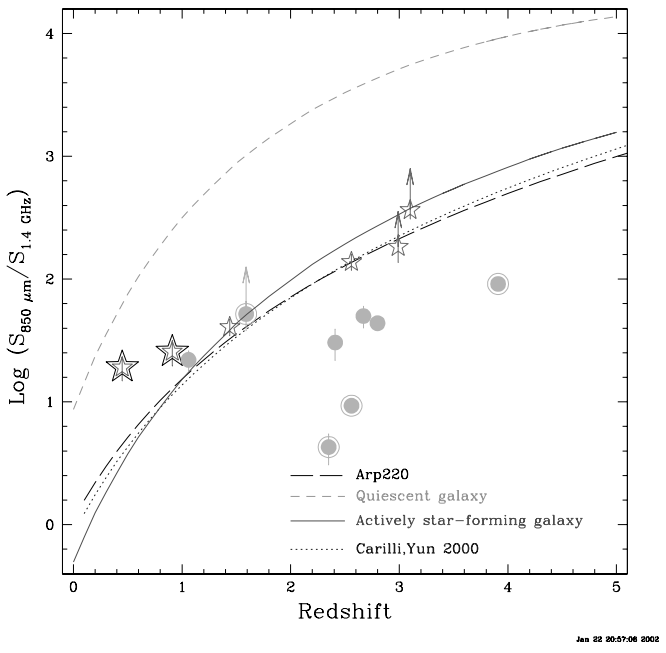

FIG. 5.—850 μm/1.4 GHz ratio as a function of redshift for galaxies of various activity levels, ranging from normal spirals to starbursts, with the Carilli & Yun (2000) relation shown for ULIRGs. Our two cold FIRBACK sources are shown as double stars. Other stars depict submillimeter sources with no sign of AGN activity (in increasing redshift order: HR 10 Dey et al. 1999; SMM J14011+0252, Ivison et al. 2001; westphal MMD 11, Chapman et al. 2002b; SSA 22 blob1, Chapman et al. 2001). For comparison, we plot four submillimeter-selected sources identified as AGNs with circles (Smail et al. 2002) and four submillimeter-detected BAL quasars with double circles (Lewis & Chapman 2002).

such cooler, luminous sources may affect seriously the interpretation of the high-redshift, SCUBA-selected population (see also Eales et al. 2000).

Cold yet luminous dusty sources suggest large masses of dust heated at moderate intensity, rather than small amounts of dust in a compact configuration subjected to extremely intense radiation fields. This latter scenario is clearly supported by the spatial and SED properties of the nearby ULIRG Arp 220 (Soifer et al. 1984). While one could invoke evolving or novel dust properties to explain cooler, high-luminosity sources like FN1-40 and FN1-64, there is no evidence to support such unusual dust properties, especially considering that the SEDs of both FN1-40 and FN1-64 are fitted quite well with the Dale et al. models from the local universe. For objects like FN1-40 and FN1-64, however, the data suggest a spatially distributed star formation activity heating a more extended ISM. The main difficulty, then, is to explain the high extinctions suggested by the large infrared-to-visible ratios in these systems. Since we know little of their detailed morphology or geometry, we cannot exclude the possibility that the initial conditions and the details of the encounters (strong tidal interactions, rather than direct collisions or mergers) result in obscured yet distributed, rather than strongly concentrated, star formation activity.

4.1. *Comparison with Higher Redshift SCUBA Populations*

Figure 5 shows how these FIRBACK sources compare with other submillimeter luminous sources with measured spectroscopic redshifts. Note that while the FIRBACK sources appear to be pure starburst, there are very few spectroscopically identified submillimeter galaxies at high redshift for comparison that do not show AGN signatures (SMM J14011+0252 at $z = 2.56$, Ivison et al. 2001; Westphal MMD 11 at $z = 2.99$, Chapman et al. 2002b; HR 10 at $z = 1.44$, Dey et al. 1999). Both FN1-64 and FN1-40 appear morphologically similar to the SCUBA galaxies SMM J14011+0252 and Westphal MMD 11, having a red $r-K$ source identified with the far-IR emission, along with a bluer companion. This is similar to the morphology of several local ULIRGs (e.g., 08279+1372; Surace & Sanders 1999; Goldader et al. 2002), and it may suggest that all these galaxies are generating their far-IR output by similar mechanisms.

As these two sources lie midway between the local *IRAS* population and the high-redshift, SCUBA-selected population (see, e.g., Smail et al. 2002), understanding their properties provides a crucial benchmark for continued progress on the evolution of IR-luminous galaxies. FN1-40 and FN1-64 are representative of the optically faint FIRBACK sample with radio and SCUBA detections (~30%; Scott et al. 2000), comprising ~8% of the radio-identified FIRBACK survey. In terms of the bright ($S_{850\ \mu m} > 6$ mJy), blank-field submillimeter sources (see, e.g., Smail et al. 2002; Scott et al. 2002) in this area on the sky, they would represent only a small fraction of the 850 μm counts (~3%).

The strong bias to colder dust temperatures in submillimeter- and far-IR–selected samples occurs because the selection bands fall redward of the graybody peak. At an observed 170 μm, this implies the cold bias out to $z \sim 1$ discussed above. However, for 850 μm, this bias is inherent in the entire plausible range of galaxy evolution, out to $z \sim 8$ (see, e.g., Blain 1999). In this sense, the wide-field SCUBA surveys will preferentially uncover the coldest sources for a given luminosity.

We would like to use the existence of these cold, luminous sources to place a constraint on the dust temperature distribution at high redshifts. If the important driver of the dust temperature is the radiation field, then we must compare at similar luminosity systems. Figure 4 suggests that these luminous FIRBACK sources are within the coldest 16% of the local population, if we cut at the same luminosity. If we propose that this local population of IR-luminous objects undergoes a strong luminosity evolution of the form $(1 + z)^4$ out to $z = 1.5$, we can determine the relative numbers of cold and warm objects isolated by our selection function. This form of evolution has been shown to match the observe space density of high-z ULIRGs to the local population (see, e.g., Blain et al. 1999; Chapman et al. 2002a).

We start with the FIRBACK survey limit, $S_{170\ \mu m} > 120$ mJy. We add the requirement that $S_{850\ \mu m}/S_{1.4\ GHz}$ gives $(1 + z)/(T_d/50\ K) > 2$, the Carilli & Yun (2000) criterion we employed to select high-redshift objects for spectroscopic follow-up with Keck. This selection function implies that we begin to detect objects with $T_d < 30$ K at $z > 0.35$ and those with $T_d < 50$ K at $z > 1$. We find 35% more FIRBACK-detectable objects with $T_d < 30$ K than with $30\ K < T_d < 50$ K in the accessible volume from $z = 0.35$ to $z = 1.6$, where we can no longer detect a 50 K source. As our two detected sources have $T_d = 26$ and 32 K, our 35% bias toward selecting $T_d < 30$ K sources implies that the outcome of our experiment deviates by less than 1 σ from the expected outcome.

We can conclude that the dust temperature distribution at higher redshifts is consistent with that observed locally (or alternatively, that the characteristic temperature of a ULIRG does not increase dramatically out to $z \sim 1$). Note that this is not necessarily the expected result. For instance, different temperature distributions for similar-luminosity ULIRG populations at $z = 0$ and $z = 1$ could arise because of different geometry of the active region, or different chemical properties of the dust. Complete redshift distributions for the FIRBACK population will be required to carefully test the dust temperature distributions at low and high redshift. A more detailed model, taking into account the local bivariate luminosity function in L_{TIR} and $S_{60\ \mu m}/S_{100\ \mu m}$, studies directly the effect of the complete distribution of dust properties on the high-redshift, far-IR population (S. C. Chapman et al. 2002, in preparation).

5. CONCLUSIONS

We have obtained Keck spectra and UKIRT high spatial resolution near-IR imagery for two of the proposed highest-redshift sources from the FIRBACK 170 μm survey. This survey is currently the most sensitive probe of the properties of dusty galaxies at the peak of the FIRB.

We find that the redshifts of counterparts to the 170 μm sources confirm that both sources are ULIRGs, but that their redshifts are significantly lower than implied by fitting a typical ULIRG SED to their far-IR/submillimeter/radio SEDs. This indicates that they have cooler dust temperatures, $T_d \sim 30$ K, than the canonical ULIRG values ($T_d \sim 50$ K). The sources both show morphologies suggestive of early-stage mergers, similar to those of recently identified SCUBA galaxies and also of many local ULIRGs.

For FN1-40, we are able to examine optical line diagnostics in the region of far-IR emission. We measure a large, $A_V \sim 4$ mag, extinction, indicating a large correction to the Hβ-estimated SFR. The metallicity in this region, as probed by the R_{23} indicator and O III/N II ratio, is found to be typical for star-forming galaxies 2 orders of magnitude less luminous (close to solar).

The detection of these galaxies in the submillimeter by SCUBA allows a constraint on the 850 μm/1.4 GHz redshift indicator. We find a relation for these galaxies lying significantly above the relation found by Carilli & Yun (2000), because of their cooler dust temperatures. The existence of such cooler, but still luminous, sources may thus affect the interpretation of the SCUBA-selected population, if they are numerous at high redshift. Recent models of the far-IR galaxy counts, relying on the rapid evolution of a hot ULIRG component to the local luminosity function, may predict an erroneous redshift distribution without taking into account sources like FN1-40 and FN1-64.

We have turned the discovery of these two cold, luminous galaxies into an estimate for the dust temperature distribution at $z \sim 1$ for the ULIRG population. We conclude that our 170 μm, 850 μm, and 1.4 GHz selection function isolates approximately 35% more cold sources (less than 30 K) than warmer sources (30 K $< T_d <$ 50 K) over the detectable redshift range, under the assumption that the temperature distributions at $z = 0$ and $z = 1$ are similar. The relative proportion of the cold population at low and high z can therefore be understood as consistent with the local 60 μm/100 μm distribution.

Thanks to A. Blain for stimulating conversations about this source population. We acknowledge the useful comments of an anonymous referee, which helped improve the text. The Isaac Newton Telescope (INT) WFC data were made publicly available through the Isaac Newton Group's Wide Field Camera Survey Programme. The Isaac Newton Telescope is operated on the island of La Palma by the Isaac Newton Group in the Spanish Observatorio del Roque de los Muchachos of the Instituto de Astrofísica de Canarias. UKIRT is operated by the Joint Astronomy Centre on behalf of the UK Particle Physics and Astronomy Research Council. I. R. S. acknowledges support from the Royal Society and the Leverhulme Trust.

REFERENCES

Blain, A. W. 1999, MNRAS, 309, 955
Blain, A. W., Smail, I., Ivison, R. J., & Kneib, J.-P. 1999, MNRAS, 302, 632
Bridger, A., et al. 2000, Proc. SPIE, 4009, 227
Carilli, C. L., & Yun, M. S. 2000, ApJ, 530, 618 (erratum 539, 1024)
Carollo, C. M., & Lilly, S. J. 2001, ApJ, 548, L153
Chapman, S. C., Lewis, G., Scott, D., Borys, C., & Richards, E. A. 2002a, ApJ, 570, 557
Chapman, S. C., Lewis, G. F., Scott, D., Richards, E., Borys, C., Steidel, C. C., Adelberger, K., & Shapley, A. 2001, ApJ, 548, L17
Chapman, S. C., Shapley, A., Steidel, C., & Windhorst, R. 2002b, ApJ, submitted
Chary, R., & Elbaz, D. 2001, ApJ, 556, 562
Ciliegi, P., et al. 1999, MNRAS, 302, 222
Dale, D. A., & Helou, G. 2002, ApJ, in press
Dale, D. A., Helou, G., Contursi, A., Silbermann, N. A., & Kolhatkar, S. 2001, ApJ, 549, 215
Dey, A., Graham, J. R., Ivison, R. J., Smail, I., Wright, G. S., & Liu, M. C. 1999, ApJ, 519, 610
Dole, H. 2000, Ph.D. thesis, Univ. of Paris-Sud XI, Orsay
Dole, H., et al. 2000, in *ISO* Survey of a Dusty Universe, ed. D. Lemke, M. Stickel, & K. Wilkes (Berlin: Springer), 54
Dunne, L., Eales, S., Edmunds, M., Ivison, R., Alexander, P., & Clements, D. L. 2000, MNRAS, 315, 115
Eales, S., Lilly, S., Webb, T., Dunne, L., Gear, W., Clements, D., & Yun, M. 2000, AJ, 120, 2244
Fisher, K., Huchra, J. P., Strauss, M. A., Davis, M., Yahil, A., & Schlegel, D. 1995, ApJS, 100, 69
Fixsen, D. J., Dwek, E., Mather, J. C., Bennett, C. L., & Shafer, R. A. 1998, ApJ, 508, 123
Flores, H., et al. 1999, ApJ, 517, 148
Franceschini, A., Aussel, H., Cesarsky, C. J., Elbaz, D., & Fadda, D. 2001, A&A, 378, 1
Goldader, J. D., Meurer, G., Heckman, T. M., Seibert, M., Sanders, D. B., Calzetti, D., & Steidel, C. C. 2002, ApJ, 568, 651
Helou, G., Soifer, B. T., & Rowan-Robinson, M. 1985, ApJ, 298, L7
Ivison, R. J., Smail, I., Frayer, D. T., Kneib, J.-P., & Blain, A. W. 2001, ApJ, 561, L45
Jansen, R. A., Fabricant, D., Franx, M., & Caldwell, N. 2000, ApJS, 126, 331
Kobulnicky, H. A., Kennicutt, R. C., Jr., & Pizagno, J. L. 1999, ApJ, 514, 544
Lewis, G., & Chapman, S. 2002, MNRAS, submitted
Pagel, B. E. J., Edmunds, M. G., Blackwell, D. E., Chun, M. S., & Smith, G. 1979, MNRAS, 189, 95
Puget, J.-L., Abergel, A., Bernard, J.-P., Boulanger, F., Burton, W. B., Désert, F.-X., & Hartmann, D. 1996, A&A, 308, L5
Puget, J.-L., et al. 1999, A&A, 345, 29
Sajina, A., Scott, D., Borys, C., Chapman, S., Dole, H., Halpern, M., & Puget, J.-L. 2002, MNRAS, submitted
Scott, D., et al. 2000, A&A, 357, L5
Scott, S. E., et al. 2002, MNRAS, 331, 817
Smail, I., Ivison, R. J., Blain, A. W., & Kneib, J.-P. 2002, MNRAS, 331, 495
Soifer, B. T., et al. 1984, ApJ, 283, L1
Surace, J. A., & Sanders, D. B. 1999, ApJ, 512, 162
Veilleux, S., & Osterbrock, D. E. 1987, ApJS, 63, 295